Numerical Analysis of Molten Salt Spreading Using Particle Method

Wiktor Gronek and Han-Young Yoon*
Department of Nuclear Power Plant Engineering, KEPCO International Nuclear Graduate School (KINGS)
**Corresponding author: hyyoon@kings.ac.kr*

***Keywords : Molten salt, Particle method, MSR safety, NaCl-UCl3**

1. Introduction

In recent years, there has been renewed global interest in Molten Salt Reactors (MSRs) and the number of activities related to the design and technology of these reactors is growing [1]. MSRs are expected to have advantages over Light Water Reactors (LWRs) in terms of safety and are highly anticipated to exclude severe accidents such as meltdowns [2]. However, confirming the safety of MSRs requires a thorough investigation of molten salt behavior during leakage events. Understanding the spreading dynamics and subsequent solidification of spilled salt within the containment geometry is critical, as it determines the spatial distribution of radionuclide-bearing salt throughout the reactor building.

The spreading of molten salt is a free-surface flow physically similar to molten core spreading in LWRs. Given this similarity, MSR leakage analysis can utilize numerical strategies developed for corium research. In particular, Lagrangian particle methods provide an efficient approach, as they naturally capture the evolution of free surfaces and bypass the time-consuming mesh generation required for complex geometries [3-5].

Building upon the established expertise in corium spreading and recognizing the scarcity of research specifically dedicated to molten salt spreading and solidification, this study adopts a Lagrangian approach, specifically the Moving Particle Semi-implicit (MPS) method [6], to analyze molten salt spreading behavior. MPS method, specifically designed for incompressible free-surface flows, has been extended by adding a heat transfer, phase change and surface tension models. To enhance computational performance, Code C has been optimized by implementing a domain decomposition strategy into a grid-based structure, combined with parallel computing using the OpenMP framework.

The ultimate objective of this research is to validate the developed numerical model by comparing its results with the MSR Salt Spill Accident experimental data, involving eutectic NaCl-UCl3 salt, conducted by Argonne National Laboratory [7]. However, as the validation process is currently ongoing, this paper presents preliminary findings focused on the model's implementation and initial spreading simulations. While a rigorous quantitative comparison is still in progress, these results demonstrate the code's capability to capture the fundamental physics of the spill before full-scale validation is completed.

2. Numerical Methodology

The MPS method is a Lagrangian, meshless CFD approach designed to model incompressible fluids without a computational grid. Unlike Eulerian methods, MPS tracks discrete particles and their interactions within a defined effective radius.

2.1. Kernel Function

The interaction between particles is quantified by the kernel function $w(r)$ as shown in Eq. 1:

$$w(r_{ij}) = \begin{cases} \frac{r_e}{r_{ij}} - 1 & 0 \le r_{ij} < r_e \\ 0 & r_e \le r_{ij}, \end{cases} \tag{1}$$

where r_{ij} is the distance between particle i and particle j, and r_e is the effective radius. The effective radius for the particle interaction is determined by the initial particle distance l_0. In this study, r_e is set to $2.1l_0$ for the number density and the gradient operator, $3.1l_0$ for the Laplacian operator, and $3.2l_0$ for the surface tension model.

2.2. Governing Equations

The governing equations of the MPS method based on Lagrangian description are the continuity, momentum, and energy equations, which can be written as non-conservative form:

$$\frac{D\rho}{Dt} = 0 \tag{2}$$

$$\frac{D\mathbf{u}}{Dt} = -\frac{1}{\rho}\nabla P + \nu\nabla^2\mathbf{u} + \mathbf{g} + \frac{\mathbf{F_s}}{\rho} \tag{3}$$

$$\frac{DT}{Dt} = \frac{k}{\rho C_p}\nabla^2 T + Q, \tag{4}$$

where t represents time, ρ the density, $\mathbf{u}$ the velocity vector, P the pressure of the fluid, ν the kinetic viscosity, $\mathbf{g}$ the gravitational acceleration, $\mathbf{F_s}$ the surface tension force, k the thermal conductivity, T the temperature, C_p the specific heat capacity, and Q the heat source.

2.3. Pressure Gradient Term

In the MPS method, the pressure gradient acting on the particle i is discretized as:

$$\nabla P_i = \frac{d}{n_0} \sum_{j \neq i} \left(\frac{P_j - P_i}{r_{ij}^2} \mathbf{r}_{ij} w(r_{ij}) \right), \tag{5}$$

where d is the dimension number of the space, n_0 is the standard value of the particle number density, $\mathbf{r}_{ij}$ is the unit vector for the direction from particle j to particle i.

2.4. Viscosity Term

The Laplacian of the velocity vector in the viscosity term of particle i is discretized by using the weight function in the following equation:

$$\nabla^2 \mathbf{u}_i = \frac{2d}{\lambda n_0} \sum_{j \neq i} \left[(\mathbf{u}_j - \mathbf{u}_i) w(r_{ij}) \right], \tag{6}$$

where λ is a coefficient for obtaining agreement between the variance increase in the variable distribution and the analytical solution.

2.5. Surface Tension Model

For the surfacce tension calculation, the potential model proposed by Kondo et al. [8] is used. This model was further developed on the basis of the mechanism that surface tension force is actually a net force of all the intermolecular forces of all liquid molecules.

The force of surface tension $\mathbf{F}_s$ acting on particle i is defined as follows by using the potential function $\phi(r_{ij})$:

$$\mathbf{F}_s = -\sum_{j \neq i} \frac{\partial \phi(r_{ij})}{\partial r} \frac{\mathbf{r}_{ij}}{r_{ij}}. \tag{7}$$

In this study, the potential function $\phi(r_{ij})$ is defined as follows, which is the same as the function used by Kondo et al. [8]:

$$\phi(r_{ij}) = C p(r_{ij}) \tag{8}$$

$$p(r_{ij}) = \begin{cases} \frac{1}{3}(r_{ij} - \frac{3}{2} l_0 + \frac{1}{2} r_e)(r_{ij} - r_e)^2 & (r_{ij} < r_e) \\ 0 & (r_{ij} \geq r_e), \end{cases} \tag{9}$$

where C is the coefficient of the potential function. The potential force using this function acts as an attractive force while $r_{ij} > l_0$ and a repulsive force while $r_{ij} < l_0$.

2.6. Heat Transfer and Phase Change Model

Heat conduction term of right side of the Eq. 4 is calculated by MPS Laplacian model explicitly [9].

$$\frac{\partial H_i}{\partial t} = k \cdot \frac{2d}{n_0 \lambda} \sum_{j \neq i} (T_j - T_i) w(r_{ij}) + Q, \tag{10}$$

where H is the enthalpy per unit volume.

Phase transition is simulated by two types of particles, fluid particles and solid particles, differing in their thermal energies per unit volume. Temperature is the function of the thermal energy per unit volume as follows:

$$T = \begin{cases} T_s + \frac{H - H_{s0}}{C_{ps}} & (H < H_{s0}) \\ T_s & (H_{s0} \leq H \leq H_{s1}) \\ T_s + \frac{H - H_{s1}}{C_{pl}} & (H_{s1} < H) \end{cases} \tag{11}$$

where T_s is the melting temperature, H_{s0} is the enthalpy at the start of melting, H_{s1} is the enthalpy at the end of the melting point, C_{ps} is the specific heat of the solid phase, and C_{pl} is the specific heat of the liquid phase.

2.7. Algorithm of Calculations

The implemented algorithm is divided into an explicit prediction phase and an implicit pressure correction phase.

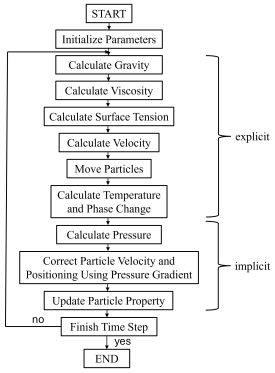

Fig. 1. Calculation flow of the MPS method.

3. Verification of Physical Models

The standard Moving Particle Semi-implicit (MPS) framework was extended by models for phase change transitions and surface tension.

3.1. Verification of Surface Tension Model

A 2D droplet oscillation case was used to verify the surface tension model. The initially square shape becomes circular due to the action of surface tension.

Table I Simulation parameters for surface tension verification

Parameter	Value	Unit
Density	798.0	$\mathrm{kg/m^3}$
Kinematic Viscosity	1.39×10^{-6}	$\mathrm{m^2/s}$
Surface Tension Coefficient	2.361×10^{-2}	$\mathrm{N/m}$
Droplet Size	0.075	m
Theoretical Oscillation Cycle	1.36	s
Particle Distance	0.0025	m
Time Step	0.002	s

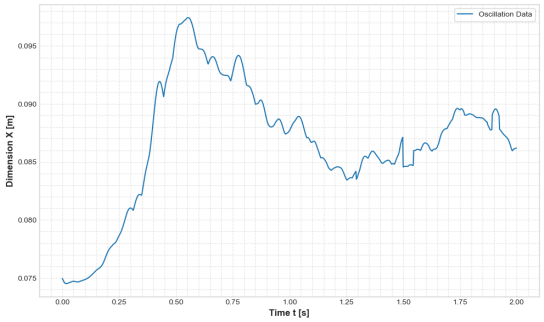

Fig. 2. Width of oscillating droplet.

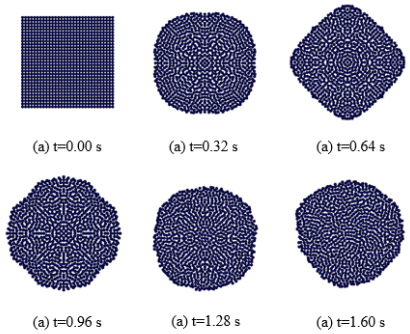

Fig. 3. Droplet oscillation.

The 2D simulation results show agreement with the theoretical droplet oscillation time. After approximately 1.3 seconds, the droplet first achieves a circular shape.

3.2. Verification of Phase Change Model

To verify the phase change model and consequently the heat transfer model, the analytical solution given by Eq. 12-14 were used.

$$T_1(t,x) = T_w + (T_m - T_w)\frac{erf\left(\frac{x}{2\sqrt{\alpha_1 t}}\right)}{erf(R)} \tag{12}$$

$$T_2(t,x) = T_\infty + (T_\infty - T_m)\frac{1 - erf\left(\frac{x}{2\sqrt{\alpha_2 t}}\right)}{1 - erf\left(R\sqrt{\frac{\alpha_1}{\alpha_2}}\right)} \tag{13}$$

$$\frac{exp(-R^2)}{erf(R)} - \frac{T_\infty - T_m}{T_m - T_w}\frac{k_2}{k_1}\sqrt{\frac{\alpha_1}{\alpha_2}}\frac{exp(-\alpha_1 R^2/\alpha_2)}{1 - erf(\sqrt{\alpha_1/\alpha_2}R)} = \frac{\sqrt{\pi}RL_{ls}}{C(T_m - T_w)} \tag{14}$$

where T_w is the temperature of the cooling surface, T_m is the melting temperature, T_∞ is the temperature at $x = \infty$, x is the distance from the cooling surface, $T_1(t,x)$ is the temperature distribution of the solid phase, $T_2(t,x)$ is the temperature distribution of the liquid phase, and R is the solution for Equation (14). L_{ls} denotes the latent heat.

Fig. 4 shows the MPS simulation of one-dimensional solidification behavior. In this simulation, the physical properties for both solid and liquid are $k = 4.0 \times 10^2$ W/(m · K), $\rho = 1.0 \times 10^3$ kg/m^3, $C = 1.0 \times 10^3$ J/(kg · K), $L_{ls} = 2.0 \times 10^5$ J/m^3, $T_w = -100$°C, $T_m = 0$°C, $T_w = 10$°C, and $R = 1.19$.

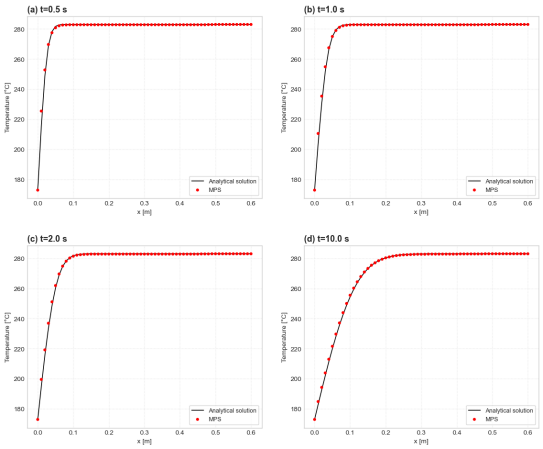

Fig. 4. Result of MPS simulation of one-dimensional solidification behavior.

The implemented phase change model accurately reflects the analytical solution, which confirms the appropriateness of its use.

4. Validation Process

Physical models implemented in the classical MPS method were verified by comparison to analytical solutions. The verified 2D models for surface tension and 1D models for phase change can be directly transferred to the 3D case. To validate the presented calculation program, the results will be compared to the experiment of spreading eutectic NaCl-UCl3 salt, conducted by Argonne National Laboratory. Molten NaCl-UCl3 was poured onto a stainless steel sheet. The top end of the catch pan was elevated to create a tilt angle of 2.5°.

Table II Simulation parameters of NaCl-UCl3 at 740 °C

Parameter	Value	Unit
Density	3295.0	kg/m^3
Kinematic Viscosity	0.823×10^{-6}	m^2/s
Surface Tension Coefficient	0.105	N/m
Thermal Conductivity	0.426	W/(mK)
Specific Heat Capacity	567.0	J/(kgK)
Latent Heat	1.58×10^5	J/kg
Temperature of Phase Change	520.0	K

To perform an MPS simulation of the MSR Salt Spill Accident experiment using the physical parameters from Table II, the maximum particle distance is 2.0×10^{-4}m. To simulate flow of 65 g of eutectic NaCl-UCl3 more than 2.47×10^6 particles are needed.

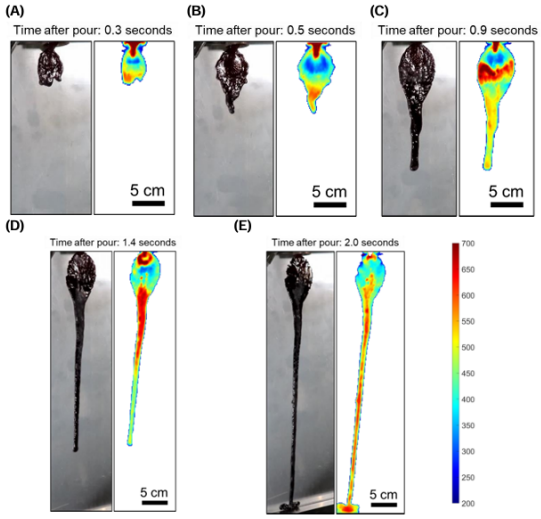

Fig. 5. Still frames from video taken by the visible and IR camera that show 65 g of eutectic NaCl-UCl3 at an initial temperature of 740 °C flowing and spreading onto a catch pan (the MSR Salt Spill Accident experiment) [7].

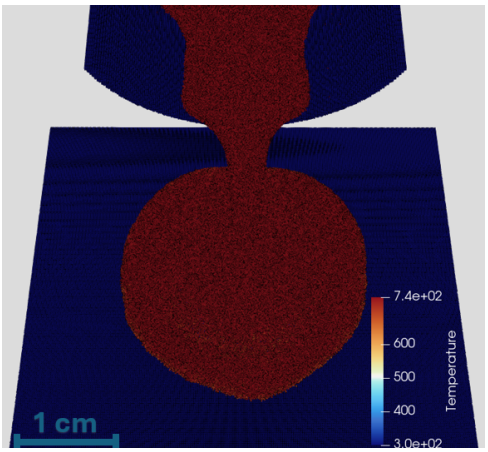

Fig. 6. Initial frame (after 0.1 s) of MPS simulation of three-dimensional molten salt spreading.

5. Conclusions

The results of the simulation indicate that the MPS method is a promising tool for predicting the free surface behavior of spreading molten salt, as demonstrated by the initial 0.1 s of the process. A key advantage of this approach is its physical accuracy, as material properties do not require manual numerical adjustments.

However, the high number of particles necessary for full-scale experiments poses a significant computational challenge. Despite implementing OpenMP parallelization and optimized neighbor searching, the current simulation time remains prohibitively long. To make the MPS method practical for larger scale applications, further software optimization and the integration of GPU-based computing are required.

Acknowledgement

This research was supported by the 2026 Research Fund of the KEPCO International Nuclear Graduate School (KINGS), the Republic of Korea.

REFERENCES

[1] IAEA, Status of Molten Salt Reactor Technology, Technical Reports Series No. 489, 2023.
[2] J. Serp, M. Allibert, O. Beneš, S. Delpech, O. Feynberg, V. Ghetta, D. Heuer, D. Holcomb, V. Ignatiev, J.L. Kloosterman, L. Luzzi, E. Merle-Lucotte, J. Uhlíř, R. Yoshioka, and D. Zhimin, The molten salt reactor (MSR) in generation IV: Overview and perspectives, Progress in Nuclear Energy, vol. 77, pp. 308–319, 2014.
[3] L. Zhao, W. Ma, and S. Bechta, Numerical study on melt underwater spreading with MPS method, Annals of Nuclear Energy, vol. 181, 109581, 2023.
[4] T. Matsuura and Y. Oka, MPS simulation of spreading behavior of molten materials, III International Conference on Particle-based Methods: Fundamentals and Applications (PARTICLES 2013), Stuttgart, Germany, 2013.
[5] G. Duan, A. Yamaji, and S. Koshizuka, A novel multiphase MPS algorithm for modeling crust formation by highly viscous fluid for simulating corium spreading, Nuclear Engineering and Design, vol. 343, pp. 218–231, 2019.
[6] S. Koshizuka and Y. Oka, Moving particle semi-implicit method for fragmentation of incompressible fluid, Nuclear Science and Engineering, vol. 123, pp. 421–434, 1996.
[7] S. Thomas, J. Jackson, Argonne National Laboratory, MSR Salt Spill Accident Testing Using Eutectic NaCl-UCl3, ANL/CFCT-22/32, 2022.
[8] M. Kondo, S. Koshizuka and M. Takimoto, A surface tension model using inter-particle potential force in Moving Particle Semi-implicit method, Transactions of The Japan Society for Computational Engineering and Science, vol. 2007, 20070021, 2007.
[9] T. Kawahara and Y. Oka, Ex-vessel molten core solidification behavior by moving particle semi-implicit method, Journal of Nuclear Science and Technology, vol. 49, no. 12, pp. 1156–1164, 2012.